Research on Maximizing Solar Spectral Transmittance Based on Particle Swarm Optimization Algorithm

Zimiao Lin

Maynooth International Engineering College, Fuzhou University, Fuzhou, Fujian, 350108, China

832201116@fzu.edu.cn

Abstract. Winter heating demands in cold regions are substantial, and solar radiation can be used as an important supplementary energy source. Improving the light transmittance of glazing systems is a key approach to increasing energy efficiency. This study aims to optimize the thickness of the three-layer glass structures and enhance sunlight transmittance in the 300–2000 nm wavelength range to maximize transmitted energy. Based on the actual solar spectral data, the thickness combinations were optimized through a global search conducted by the particle swarm optimization (PSO) algorithm. The findings show that the optimized transmittance is up to 99.83%, the average transmittance is increased by 54.74%, the visible light transmittance is increased by 32.02%, and the integrated value of multi-angle transmittance is more than 500 W/m². The results indicate that the light transmittance performance is significantly enhanced, and the stability is robust, which verifies that the PSO algorithm is suitable for the optimization of complex nonlinear optical film structures. This study provides theoretical support for the energy-saving design of buildings and provides an optimization idea for the engineering application of multi-layer optical films.

INTRODUCTION

In northern regions, the climate is cold in winter, making heating an essential requirement for daily life and resulting in significant energy consumption. In recent years, growing environmental awareness has led to the widespread acceptance of energy-saving and emission-reducing practices. People not only pay attention to various traditional heating equipment but also hope to make better use of new energy. Among these, solar radiation is a major source of energy in nature. Therefore, designing windows to maximize the transmission of solar energy into indoor spaces has become a critical focus. However, the light transmission and reflectivity of ordinary single-layer glass are fixed, making it difficult to transmit energy efficiently. In contrast, multi-layer glass is more effective in controlling solar transmission [1].

This multi-layer glass structure can be expanded into a typical multi-layer film system and has been widely used in optical designs. Lei Wang used genetic algorithm and transfer matrix method (TMM) to design multi-layer film structure composed of high-temperature resistant materials, while Alexander Luce and Anqing Jiang further applied the TMM to reinforcement learning, combining automatic differentiation and material generation algorithm, respectively [2-4]. Xiang Li and Younis A. Yiunis both used Macleod optical design software to simulate and optimize multilayer film structures [5, 6]. The former achieved a transmittance of up to 95.3%, while the latter also achieved a high transmittance of 98% for near-infrared filter structures. Haozhu Wang proposed an optical multi-layer proximal policy optimization (OML-PPO) method based on deep reinforcement learning [7]. The results showed that the average absorption rate was as high as 99.24%, and the visible light enhancement factor was increased by 8.5%. Preetam Kumar and others used the Tandem neural network architecture (TNN) to achieve the reverse design of multilayer thin films based on TiO_2-SiO_2 materials [8]. In the test, the transmittance error was less than 20%. Ze Dong Saw and others used large language models (LLMs) to develop an optical thin film design framework based on natural language input [9]. Taigao Ma further proposed the neural network-driven OptoGPT model [10]. The results showed that each design took only about 0.1 seconds. The GLSIM program (glazing simulator) was employed by Wycliffe M. Isoe and others for optical simulation, which led to a notable increase in

energy conversion efficiency to 28.72% [11]. The above studies show that multilayer film systems have excellent spectral control capabilities and can achieve high transmittance through structural optimization, which has significant advantages in improving energy efficiency.

In summary, most of the existing research focuses on the design of specific optical components such as filters, ultra-wideband absorbers, or laser reflectors, and there are relatively few studies on their application in the field of building energy conservation. In addition, the methods used in existing studies are usually computationally intensive and complex in structure, which is not conducive to practical implementation. In order to fill these gaps, this study uses particle swarm optimization, an efficient and simple heuristic optimization algorithm, to improve the transmittance of sunlight in the wavelength range of 300nm to 2000nm, thereby reducing winter heating energy consumption, which is in line with the concept of low-carbon development and opens up a new direction for the integration of optical design and building energy conservation.

METHODOLOGY

Particle Swarm Optimization algorithm

Particle Swarm Optimization (PSO) is a heuristic algorithm inspired by the collective behavior of biological groups [12]. Unlike traditional methods, it can effectively solve complex, nonlinear problems without requiring the objective function to be continuous or differentiable [13]. PSO is also known for its simple structure, few parameters, and fast convergence.

The algorithm mimics how birds cooperatively search for food, abstracting this into a computational model that explores the solution space [14]. Each particle represents a potential solution and adjusts its velocity and position based on its personal best (pbest) and the global best (gbest), as defined by the update rules:

$$v_{i,d}^{k+1} = \omega v_{i,d}^{k} + c_1 r_1 \left(pbest_{i,d} - x_{i,d}^{k}\right) + c_2 r_2 \left(gbest_{d} - x_{i,d}^{k}\right) \quad (1)$$

$$x_{i,d}^{k+1} = x_{i,d}^{k} + v_{i,d}^{k+1} \quad (2)$$

Here, $v_{i,d}^{k+1}$ and $x_{i,d}^{k+1}$ are the updated velocity and position of particle i in dimension d at iteration $k+1$. The inertia weight ω maintains momentum, while c_1 and c_2 control individual and social learning. Random factors r_1 and r_2 (in [0, 1]) add diversity to avoid premature convergence.

In practical applications, PSO is also affected by the following parameters. The number of particles, that is, the population size, determines the coverage of the search space. This study selected 20 particles, which can ensure the search capability while taking into account the computational efficiency [15]. The iteration limit affects the depth of the search. Setting it too small may lead to early convergence, while setting it too large will increase the computational cost. This study sets the number of iterations to 300, which is a value adapted to the complexity of the problem. In addition, the boundary of the speed update is also an important control factor. A larger speed boundary is conducive to global search, but it is easy to cross the optimal area. A smaller speed boundary is conducive to fine search, but increases the risk of getting trapped in suboptimal solutions [16, 17]. This study sets the maximum speed to 0.5, which can achieve a good balance between global exploration and local development.

Transmittance Calculation

When a beam of light enters a single-layer glass film with a refractive index of n, the light is reflected and transmitted multiple times at the interfaces on both sides of the glass film. The incident light is refracted when it first enters the glass layer, forming the first beam of transmitted light; the rest of the light propagates back and forth between the upper and lower interfaces at an angle θ in the glass. Each time reflection and transmission occur at the interface, this process is repeated continuously, resulting in a series of coherent multiple reflected light waves and transmitted light waves in the glass layer [18]. Each beam of transmitted light is accompanied by a certain phase delay relative to the previous beam. The first beam of transmitted light is $tt'A_i$, and the amplitude of each subsequent round-trip reflection is $tt'r^2A_ie^{-i\delta}$, $tt'r^4A_ie^{-2i\delta}$, etc. By adding the transmission amplitudes of each order, the total transmission complex amplitude A_t can be expressed as:

$$A_t = tt'A_i + tt'r^2A_ie^{-i\delta} + tt'r^4A_ie^{-2i\delta} + \cdots \quad (3)$$

Where t and t' are complex transmission coefficients, r is the reflection coefficient, δ is the optical path difference of a single round trip, defined as:

$$\delta = \frac{4\pi nl\cos\theta}{\lambda} \quad (4)$$

Assume that the incident light is incident from a medium with a refractive index of n_0 (such as air) into a single layer of glass with a refractive index of n, whose thickness is l, the incident angle is θ, and the wavelength is λ. Define $tt' = T$, $r^2 = R$, and the transmittance expression is:

$$T = \frac{I_t}{I_i} = \frac{(1-R)^2}{(1-R)^2+4R\sin^2\left(\frac{\delta}{2}\right)} \quad (5)$$

Wherein, $R = \left(\frac{n-n_0}{n+n_0}\right)^2$ is the reflectivity, and I_i、I_t are the intensities of incident light and transmitted light, respectively.

After obtaining the calculation formula for the transmittance of a single layer of glass, it can be further extended to the three-layer glass model of this study. Each layer of glass has the same refractive index n, and the thicknesses are l_1, l_2, and l_3 respectively. The optical path difference of each layer is recorded as δ_1, δ_2, and δ_3 respectively, which can be calculated according to formula (4). For each layer, the transmittance T_1, T_2, and T_3 are calculated based on formula (5), and then the total transmittance of the overall structure is obtained as the product of the transmittances of the three layers. The final total transmitted light intensity I_{trans} is obtained by multiplying the original irradiance intensity I_{in} of the solar spectrum by the total transmittance of the structure:

$$I_{trans} = I_{in} \cdot T_1 \cdot T_2 \cdot T_3 \quad (6)$$

Optical Modeling Process

This study built a transmittance optimization model for a three-layer glass structure on MATLAB software. The refractive index of each layer of glass was set to the same value, and the thickness of each layer was set to 3 mm to 10 mm. To simulate more realistic lighting conditions, this study selected the international standard solar spectrum data, namely the full spectrum irradiance data in ASTM G173-03, which can fully reflect the transmittance characteristics of solar energy at different wavelengths [19]. Considering that the incident angle changes continuously in real application scenarios, the study introduced multiple incident angles, calculated the total transmittance at each angle, and comprehensively evaluated the optical performance of the three-layer structure.

RESULTS AND DISCUSSION

Results Analysis

After 300 iterations of the PSO algorithm, the optimal thickness values for the inner, middle, and outer layers were found to be 5.09 mm, 4.31 mm, and 4.97 mm, in that order. To assess the optical behavior of the multilayer design under varying angles of incidence, spectral transmittance curves were generated for angles ranging from 0° to 75° in 15° increments, as illustrated in Figure 1. Subfigures (a) to (f) correspond to different angles. The x-axis denotes the wavelength range (300–2000 nm), and the y-axis indicates solar transmission.

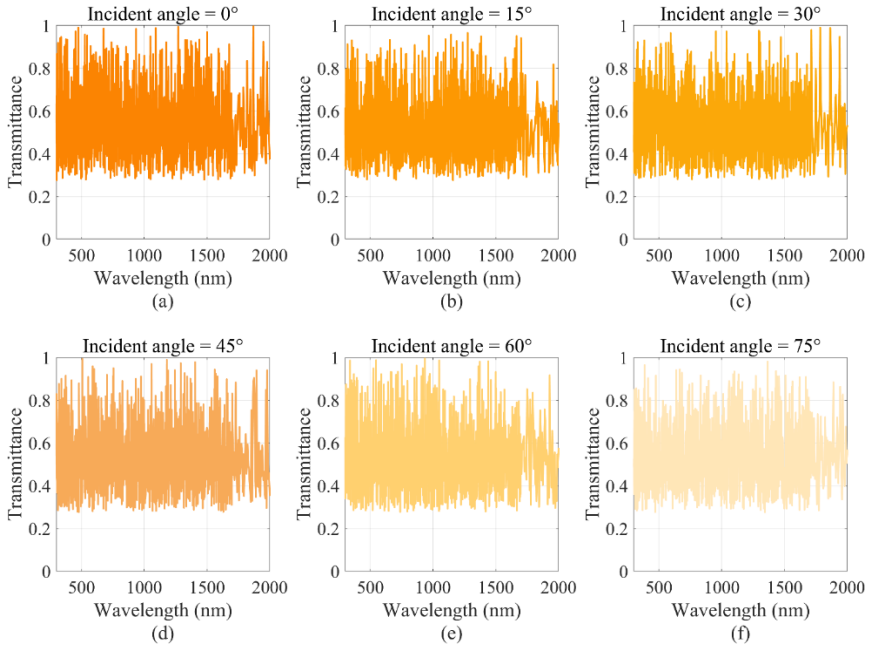

FIGURE 1. Spectral transmittance curves under varying incident angles (Original)

To more intuitively present the transmission performance indicators at various incident angles, Table 1 lists the maximum transmittance, average transmittance, 400-800nm transmittance, and total integrated value of transmitted light intensity at the corresponding angles.

TABLE 1. Transmission performance under varying incident angles (Original)

Incident Angle	Maximum Transmittance	Average Transmittance	400-800nm Transmittance	Total Transmitted Intensity (W/m^2)
0°	99.83%	54.08%	53.77%	524.19
15°	97.15%	51.96%	51.51%	502.03
30°	97.37%	52.90%	53.22%	511.31
45°	98.82%	52.47%	52.51%	506.49
60°	98.55%	53.75%	53.84%	519.00
75°	97.54%	52.56%	52.20%	508.25

Combining Figure 1 with Table 1, it can be seen that under vertical incidence (0°), the transmittance is maintained at a medium-high level in the entire band, with the highest transmittance reaching 99.83% at 483nm, close to the theoretical limit. As the angle increases, the overall level of transmittance decreases slightly, and the fluctuation increases, especially in the short-wave band (300-800 nm), indicating that the system's transmission efficiency for oblique incident light is weakened. Although the transmittance curves at different angles fluctuate in detail, the overall trend is consistent, and the maximum transmittance is always maintained above 97.00%. The weighted average transmittance and the transmittance in the visible light band change little, and have good stability to changes in the incident angle.

Figure 2 below shows the transmitted light intensity curves at different incident angles under the optimal thickness combination:

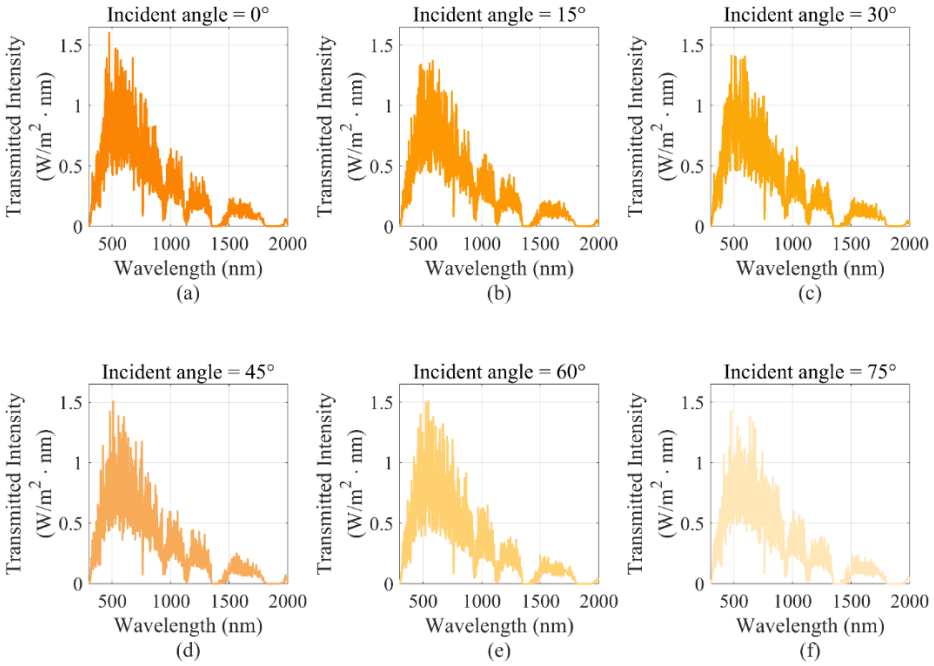

FIGURE 2. Transmitted light intensity curves under varying incident angles (Original)

As can be seen from Figure 2, the transmittance is optimal at vertical incidence. With the gradual increase in the incident angle, the overall transmitted light intensity shows a downward trend, but the spectral distribution shape of the curve is roughly the same at different angles, and the main peak is still concentrated in the visible light band, indicating that the optimized three-layer structure has stable spectral selectivity and can consistently filter out solar energy in a specific wavelength band. As the incident angle increases, the total integral of the transmitted light intensity decreases from 524.19 W/m² to 508.25 W/m², showing a trend of first decreasing and then slowing down, and an overall downward trend. The integral values at all angles are all above 500.00 W/m², accounting for more than half of the total incident light intensity of the full band of ASTM G173, and a high energy transmission efficiency has been achieved.

Figure 3 shows the performance comparison before and after optimization in terms of maximum transmittance, average transmittance, and visible light transmittance. Each group of bar charts in the figure contains two types of data, representing the initial and optimized light transmittance performance, respectively. The x-axis represents the performance metric type, while the y-axis shows the corresponding transmittance percentage.

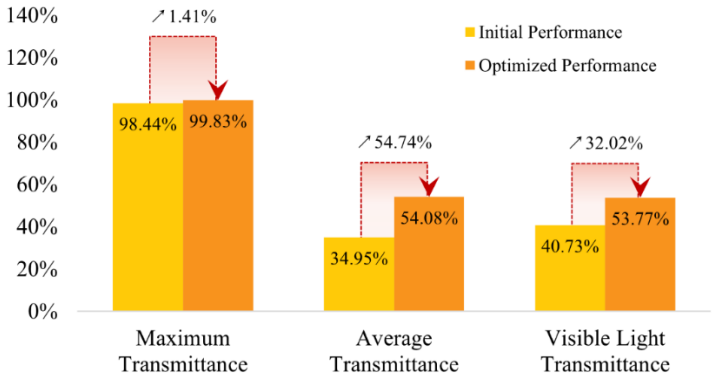

FIGURE 3. Comparison of transmittance before and after optimization under normal incidence (Original)

As illustrated in Figure 3, the average transmittance increased from 34.95% to 54.08%, representing a 54.74% improvement; the visible light transmittance increased from 40.73% to 53.77%, an increase of 32.02%. Although the

increase in the maximum transmittance is relatively small, from 98.44% to 99.83% (an increase of 1.41%), its value itself is close to the theoretical upper limit. The above results fully demonstrate that the optimized light transmittance performance is significantly improved, verifying that the method proposed in this study is effective in improving the efficiency of light energy utilization.

Discussion

To maximize solar transmittance, the thicknesses of the three-layer glass were optimized with the PSO algorithm in this study. From the final thickness combination (L_1 = 5.09 mm, L_2 = 4.31 mm, L_3 = 4.97 mm), the three-layer thicknesses showed a certain degree of symmetry and similarity, which may help to form a multiple interference enhancement effect within a certain band range, thereby improving the overall transmittance performance. However, despite the very high peak transmittance, the overall weighted average transmittance did not exceed 60%. Compared with existing studies, this phenomenon may be because there are still a lot of dramatic fluctuations in the transmittance curve. These fluctuations result from the interference enhancement and weakening of different wavelengths between multi-layer films, which leads to a significant decrease in the transmittance of certain bands and the formation of strong interference fringes [20]. It may also be that the current algorithm is more inclined to enhance the transmission peak in a few bands to obtain the optimal solution in the integral sense, without suppressing the fluctuations caused by interference.

The limitation of this study is that it assumes that the refractive index of the material is constant and does not consider complex optical effects such as the dispersion effect and factors such as scattering and surface roughness of actual glass, which may deviate from the real environment [21]. Secondly, the current goal is to maximize the intensity of transmitted light in the entire band, without comprehensively considering that poor glass insulation performance may lead to indoor heating loss in winter, and excessive ultraviolet radiation may harm human health. Although this study traverses multiple incident angles, it is not calculated based on the real environment, and the actual lighting environment is more complex.

Given the above limitations, future research can be expanded and improved in the following directions: first, the dispersion model and interface scattering effect can be introduced; second, the transmittance and thermal insulation can be comprehensively optimized by combining multi-objective optimization algorithms to achieve high visible light transmittance, infrared blocking, and ultraviolet suppression, to ensure comfort while saving energy [22]. It is also possible to consider using parallel computing or proxy models such as neural networks to improve operating efficiency [23]. In the future, the changes in solar altitude angle throughout the day/year can be simulated, and combined with building environment simulation software, the actual energy-saving benefits of the optimized structure in different geographical locations and seasons can be evaluated.

CONCLUSION

This study successfully achieved the thickness optimization design of the three-layer glass structure through the particle swarm optimization algorithm. The optimized structure showed excellent optical performance, with an average transmittance increase of up to 54.74%, and a significant increase of 32.02% in the visible light region. The evaluation indicators of multiple dimensions, such as maximum transmittance, average transmittance, visible light transmittance, and total transmitted light intensity, were used to comprehensively analyze the performance, which effectively verified the effectiveness of the PSO algorithm in solving high-dimensional nonlinear optical optimization problems. In addition, this study has good material versatility. The entire research framework does not rely on specific materials. The impact of different materials can be evaluated by modifying the corresponding parameters, providing a reliable theoretical reference for the intelligent design of multi-layer optical structures. The research results have a wide range of application values in photovoltaic building integration, greenhouses, energy-saving curtain walls, and so on, and hold significant theoretical and practical value in improving the efficiency of sunlight utilization and advancing the development of green buildings.

Future research can seek a better balance between multiple indicators such as light transmittance, thermal insulation, and structural strength to meet the comprehensive needs of different scenarios. Meanwhile, advanced methods such as machine learning can be incorporated to enhance optimization efficiency and solution adaptability, enabling the intelligent design of more complex structures. Further studies should investigate the response characteristics of multi-layer optical glass structures under varying incident angles and environmental conditions.

These efforts can promote their application in practical engineering, lay a solid foundation for the industrialization of green energy-saving materials, and contribute to achieving building energy efficiency and carbon neutrality goals.

REFERENCES

1. Y. Liu, W. Weng, C. Wang, L. Fu and Y. Tang, China Water Transport (Second Half of the Month), **3**, 232–235 (2020).
2. L. Wang, Y. Yang, X. Tang, B. Li, Y. Hu, Y. Zhu, H. Yang, Optics Letters, **46**, 5224–5227 (2021).
3. A. Luce, A. Mahdavi, F. Marquardt, H. Wankerl, Journal of the Optical Society of America A, **39**, (2022).
4. A. Jiang, L. Chen, O. Yoshie, "OTF Gym: A Set of Reinforcement Learning Environment of Layered Optical Thin Film Inverse Design," in *2021 Conference on Lasers and Electro-Optics*, pp. 1–2.
5. X. Li, L. Shen, J. Song, J. Chen, "Preparation of MgF_2, SiO_2 and TiO_2 optical films," in *2022 2nd International Conference on Consumer Electronics and Computer Engineering*, pp. 690–693.
6. Y. Yiunis, M. Yaseen, K. Mohamed, "Design of near infrared band pass multilayer thin film filter," in *2022 International Congress on Human-Computer Interaction, Optimization and Robotic Applications*, pp. 1–8.
7. H. Wang, Z. Zheng, C. Ji and L. Guo, Machine Learning: Science and Technology, **2**, 025013 (2021).
8. P. Kumar, F. Mihret, A. Mishra, E. Shivaleela, T. Srinivas, "Inverse design of multilayer thin film by deep neural network," in *2022 International Conference on Numerical Simulation of Optoelectronic Devices*, pp. 129–130.
9. Z. D. Saw, E. J. Q. Wang, Z. Yang, V. P. Bui, C. E. Png, "Knowledge-based extraction for inverse design of optical thin-films," in *TENCON 2024 – 2024 IEEE Region 10 Conference*, pp. 285–288.
10. T. Ma, M. Ma, L. Guo, iScience, **28**, 112222 (2025).
11. W. Isoe, M. Mageto, C. Maghanga, M. Mwamburi, B. Odari, Scientific African, **20**, e01678 (2023).
12. J. Kennedy, R. Eberhart, "Particle swarm optimization," in *Proceedings of ICNN'95–International Conference on Neural Networks*, pp. 1942–1948.
13. J. Nan, "PSO-BP Neural Network Based Prediction Study for Nonlinear Problems," in *2023 IEEE International Conference on Electrical, Automation and Computer Engineering*, pp. 1507–1512.
14. J. Wei, Y. Gu, K. Law, N. Cheong, "Adaptive Position Updating Particle Swarm Optimization for UAV Path Planning," in *2024 22nd International Symposium on Modeling and Optimization in Mobile, Ad Hoc, and Wireless Networks*, pp. 124–131.
15. G. R. Cai, S. L. Chen, S. Z. Li, W. Z. Guo, "Study on the Nonlinear Strategy of Inertia Weight in Particle Swarm Optimization," in *2008 Fourth International Conference on Natural Computation*, pp. 683–687.
16. M. Jain, V. Saihjpal, N. Singh, S. Singh, Applied Sciences, **12**, 8392 (2022).
17. X. Li, D. Wu, J. He, M. Bashir, L. Ma, Journal of Control Science and Engineering, **2020**, 3857894 (2020).
18. Q. Liang, *Physical Optics* (Publishing House of Electronics Industry, Beijing, 2008), Chapter 4.
19. National Renewable Energy Laboratory- NREL Solar Spectra, 2025, Available at https://www2.nrel.gov/grid/solar-resource/spectra
20. Z. Fu, Z. Cheng, F. Wang, et al., *Optik*, **289**, (2023).
21. I. Malitson, Journal of the Optical Society of America, **55**, 1205–1208 (1965).
22. K. Deb, A. Pratap, S. Agarwal, T. Meyarivan, *IEEE Transactions on Evolutionary Computation*, **6**, 182–197 (2002).
23. J. Tian, Y. Li, L. Zhang, Z. Liu, Industrial and Mining Automation, **49**, 67–74 (2023).